Available online at www.sciencedirect.com
ScienceDirect
Composite Structures 81 (2007) 303–311
COMPOSITE STRUCTURES
www.elsevier.com/locate/compstruct

Initiation and progression of composite patch debonding in adhesively repaired cracked metallic sheets

P. Papanikos [a,*], K.I. Tserpes [b], Sp. Pantelakis [c]

[a] Department of Product and Systems Design Engineering, University of the Aegean, Ermoupolis, Syros 84100, Greece
[b] Institute of Structures and Advanced Materials (ISTRAM), Patron-Athinon 57 Street, Patras 26441, Greece
[c] Laboratory of Technology and Strength of Materials, Department of Mechanical Engineering and Aeronautics, University of Patras, Patras 26500, Greece

Available online 30 October 2006

Abstract

Failure analysis of composite bonded repairs in cracked metallic structures is often given superficial treatment. Apart from crack growth, which is prevented during the design of the repair by ensuring that the stress intensity factor will remain in safe levels, patch debonding is a very critical failure mode since its presence reduces the effective area of the patch. In this paper, a finite element-based progressive failure model was used to investigate the geometrical effects on patch debonding initiation and progression induced by mechanical loading. A metallic sheet containing a central through-thickness crack loaded in tension and repaired using a double-sided rectangular tapered composite patch was used as the basic configuration. In all cases examined, the debonding is due to cohesion or adhesion failure caused by high shear stresses. It was found that, depending to the patch thickness, the debonding initiates either at the upper patch edge (being catastrophic for the repair) or at the crack faces (being not catastrophic). Given the adhesive shear strength, the debonding initiation load increases significantly with increasing the patch thickness, adhesive thickness and tapered length. Based on these findings, specific suggestions for the enhancement of composite bonded repairs against debonding are made.

Keywords: Bonded repair; Composite patch; Finite element analysis (FEA); Stress intensity factor (SIF); Progressive failure analysis

1. Introduction

The continuous growth in air transport has stimulated an increasing demand in the aeronautic industry to improve the maintainability and sustain the reliability of civil aircrafts. The best way to achieve this goal is to improve the current repair techniques and develop new ones [1]. Adhesively bonded composite patches have been established as the most effective repair method of damaged (cracked or corroded) airframes offering many advantages over the traditional method of mechanical fastened doublers including improved fatigue behavior, resistance to corrosion and minimization of stress concentration. Although implementation of composite bonded repairs started more than 30 years ago by the Royal Australian Air Force [2], at present, such repairs are certified for use only on secondary structural parts of the airframe [1]. In order to expand their use on primary structural parts also, a detailed knowledge of their mechanical performance under several loading conditions is required. Currently, this task is being mainly accomplished through very expensive and time-consuming experimental programs performed by the airline companies and research institutes under the guidance of national Air Forces.

Numerical analysis is a powerful tool, which can provide very useful information regarding the mechanical performance of composite bonded repairs. However, to date, numerical models have been only used for calculating the stress field of the repairs and optimising the patch geometry with regard to the reduction of stress intensity factor (SIF). An important, but overlooked area is failure analysis of the repairs. Designs that ignore certain critical failure modes may cause greater damage than the original damage they

* Corresponding author. Tel.: +30 22810 97100; fax: +30 22810 97109.
E-mail address: ppap@syros.aegean.gr (P. Papanikos).

0263-8223/$ - see front matter © 2006 Elsevier Ltd. All rights reserved.
doi:10.1016/j.compstruct.2006.08.022

are intended to repair. Fig. 1 illustrates the failure modes that might occur in a bonded repair of a cracked fuselage skin [3]. These are crack growth, patch debonding and nucleation of new fatigue cracks in the skin at the patch edges. The foremost failure mode is crack growth. Of almost the same importance is patch debonding, since its presence increases the possibility of crack growth in the repaired structure by reducing the effective area of the patch, and thereby, the amount of stresses being transferred from the cracked structure to the patch. Mechanically induced patch debonding may be due to either high adhesive shear stresses or high peel stresses In Fig. 2, a schematic representation of the shear stress distribution in a bonded repair is given. As can be seen, the stresses are maximized on either side of the crack and at patch edges. A standard practice for reducing the stresses at patch edges is patch tapering.

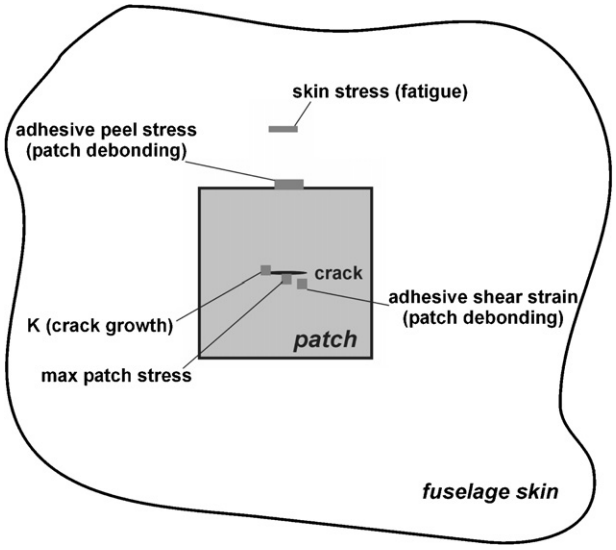

Fig. 1. Schematic of the failure modes occurring in a bonded repair of a cracked fuselage skin, after [3].

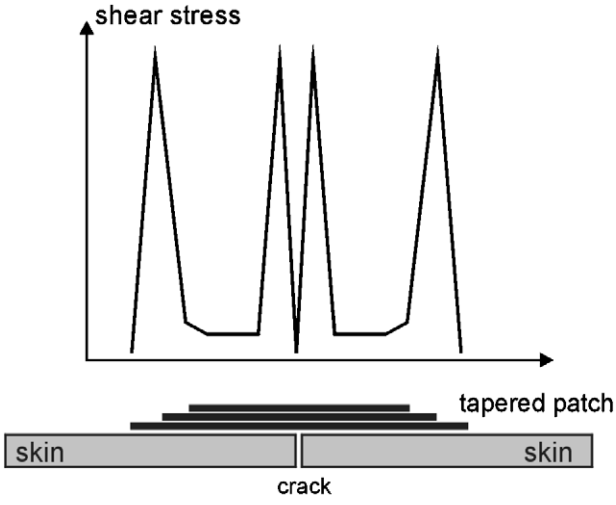

Fig. 2. Schematic of the shear stress distribution in a bonded repair, after [3].

Up to the present time, very few works have studied composite patch debonding in adhesively bonded repairs. Naboulsi and co-workers, in a series of papers [4–6], used the three-layer technique (two-dimensional FE model consisting of three layers) accompanied by experiments to investigate the effects of pre-existing debonding of various sizes and in various locations on the fatigue crack growth and life of repaired cracked structures. The results of their investigation showed a clear variation in fatigue life and SIF with varying the location and size of debonding. Recently, Megueni et al. [7] and Ouinas et al. [8] used the FE analysis to compute the SIF in cracks repaired by composite bonded patches taking into account pre-existing debonding. They also found that the presence of debonding increases the SIF considerably. Therefore, from the above works it is concluded that the presence of debonding significantly affects the effectiveness of the repairs.

It is evident that the research conducted so far on patch debonding intended to assess the importance of this failure mode. Having established the importance of debonding, the next step is to enhance the repairs against it. To this end, information is required regarding the initiation and progression of patch debonding and how specific features of the repair such as geometry and materials used may influence patch debonding. The aim of this paper is to contribute towards this objective.

2. Progressive failure analysis

The technique of progressive failure analysis has been extensively used in the past to simulate the mechanical behavior of composite bolted joints [9–11]. The authors of this paper were the first to apply this technique in composite bonded repairs in [12] by appropriately modifying a 3-D progressive failure model initially developed for composite bolted joints. The progressive failure model (PFM), used to accomplish the current study, integrates the components of *stress analysis*, *failure analysis* and *material property degradation*.

2.1. Stress analysis

Stress analysis of the repair was performed using 3-D FE models developed with the commercial FE code ANSYS [13]. The metallic sheet, composite patch and epoxy adhesive were modelled as different bodies using the 8-noded 3-D ANSYS SOLID45 element. The patch lay-up is the unidirectional $[0°]_8$. Due to symmetry of geometry and loading only one-eighth of the repair was modelled. Fig. 3 shows the FE meshes of the repair parts and complete repair. A fine mesh was adopted in the area around the crack tip to allow a satisfactory accuracy in SIF calculation. It should be noted, however, that the goal of this work is not the accurate calculation of SIF

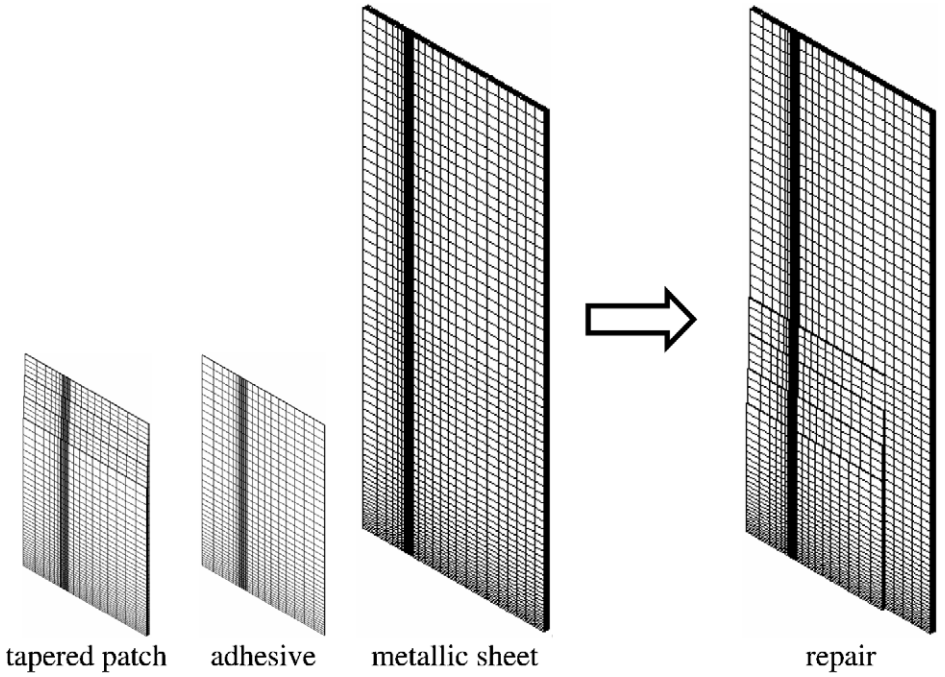

Fig. 3. FE meshes of the repair parts and complete repair.

values but, rather, the influence of repair parameters on SIF values. To this end, the mesh selected provided reasonably good results in reasonable time. Away from the crack tip, a coarser mesh was adopted in order to reduce the total number of elements. As can be seen in the close-view of the repair bottom, shown in Fig. 4, through the thickness of the sheet, patch and adhesive, four, four and one elements have been respectively used. The use of many elements through the thickness provides greater accuracy in the calculation of through thickness stresses, which are important in the prediction of patch debonding. The incremental tensile loading was applied in the sheet through the application of an incremental uniform tensile stress σ at its top surface.

2.2. Failure analysis

Failure analysis concerned both the composite patch and the adhesive. Initially, seven failure modes, representing the basic failure modes of the composite material, have been considered for the composite patch. However, the first few analyses revealed that the stress state developed in the composite patch for the specific combination of repair configuration and loading conditions was too low to cause significant failure in the patch. Based in this finding, in order to reduce the total computational effort, no failure checks were performed for the composite patch. For the adhesive and the adhesive/metal or adhesive/patch interface, three major failure modes were considered; namely, adhesive shearing, adhesive/metal peeling and adhesive/patch peeling. The failure criteria used for the detection of these failure modes are:

Adhesive shearing:

$$\tau_{\max} = \frac{\sigma_1 - \sigma_3}{2} \geqslant p_s \tag{1}$$

Adhesive/metal peeling, for ($\sigma_{za} > 0$):

$$\sigma_{za} \geqslant p_{xm} \tag{2}$$

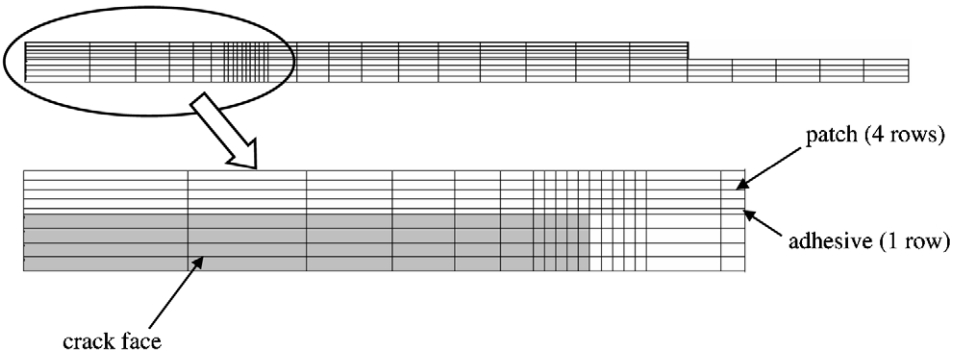

Fig. 4. Close-view of the FE mesh in the repair bottom.

Adhesive/patch peeling, for ($\sigma_{za} > 0$):

$$\sigma_{za} \geqslant p_{ap} \tag{3}$$

where τ_{max} is the maximum shear stress in the adhesive, σ_1 and σ_3 are the maximum and minimum principal stresses, and σ_{za} is the stress in the normal direction. p_s is the shear strength of the adhesive and p_{am}, p_{ap} are the peeling strengths of the adhesive/metal and adhesive/patch interfaces, respectively. To account for the shearing failure of the two interfaces, p_s can be considered as the minimum of the shear strength of the adhesive and the shear strengths of the interfaces. From the modeling point of view, this consideration seems satisfactory, since the breakage of a single element of the adhesive is equivalent to the debonding of the either of the interfaces in this element.

2.3. Material property degradation

Once failure is detected in the adhesive, material property degradation is applied by setting the elastic moduli of the failed elements equal to zero. In order to avoid numerical problems that will cause the zero values of the elastic moduli in the solution of the FE model, a very small value (=0.001 of the initial value) is set instead of zero.

2.4. Model algorithm

The three model components integrate in an iterative algorithm, which is described by means of the flowchart depicted in Fig. 5. The steps of the algorithm are numbered according to the sequence of their implementation. Note that due to the local character of the stress concentration, the criterion used in this study for examining the re-distribution of stresses at the same load level (more than 1% increase of the debonded area between two consecutive iterations, step 8 in the algorithm) may be large and a smaller value may show a slightly different debonding behaviour. However, this would increase dramatically the computational time and storage requirements. To implement the model, the ANSYS macro-language [13] was used.

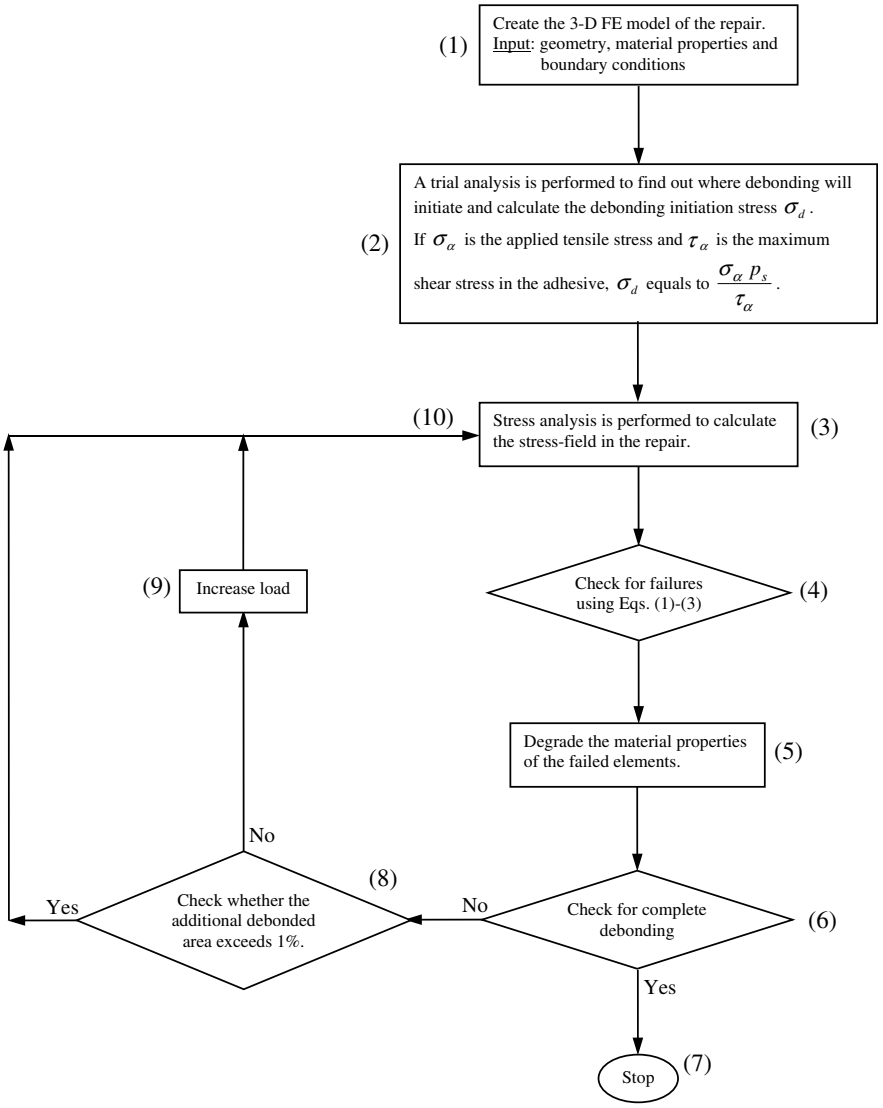

Fig. 5. Flowchart of the progressive damage model.

3. Geometrical effects

The configuration considered comprises a metallic sheet with a central through-thickness crack loaded in tension and repaired using a double-sided rectangular (symmetric) carbon-fiber-reinforced plastic (CFRP) patch with tapered edges. The dimensions of the repair parts are listed in Table 1. Except where mentioned, these dimensions were used. The material properties of the repair parts are: Aluminum sheet: $E = 70$ GPa, $v = 0.33$; CFRP patch: $E_{xx} = 168$ GPa, $E_{yy} = E_{zz} = 10$ GPa, $G_{xy} = G_{xz} = 8$ GPa, $G_{yz} = 4$ GPa, $v_{xy} = v_{xz} = 0.02$, $v_{yz} = 0.48$; Adhesive (Epoxy film FM-73): $E = 2.2$ GPa, $v = 0.35$. The subscripts in the material properties of the CFRP material refer to a local coordinate system in which the x and y-axes are parallel and transverse to the fibers, respectively, while the z-axis coincides to the normal direction. The orientation of the system was chosen such as the fibers to be oriented perpendicular to crack line.

The first few trial analyses have indicated two candidate areas for patch debonding initiation; namely, the area just above the crack (crack region) and the upper patch edge: areas A and B, respectively, in Fig. 6. Determinant about where patch debonding will initiate is the geometry. Based on this finding, a parametric study was conducted to ascertain the role of repair geometry (patch thickness and width, adhesive thickness and tapered length) in patch debonding initiation and progression.

Table 1
Dimensions of the repair parts

Dimension	Value (mm)
Sheet height	310
Sheet length	108
Sheet thickness, t_s	3
Crack length	15
Patch width (parallel to crack line)	45
Patch height (including tapered)	67
Adhesive thickness	0.15
Tapered length	20

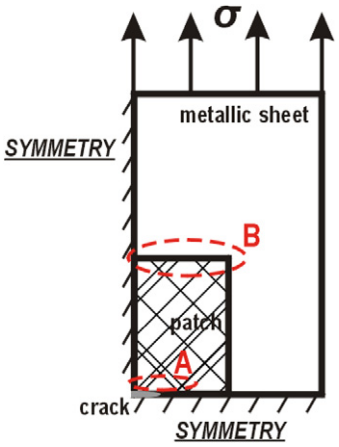

Fig. 6. Candidate areas for patch debonding initiation.

3.1. Effect of patch thickness

Fig. 7 shows the variation of debonding initiation stress σ_d normalized by the shear strength p_s at the areas A and B as function of the patch thickness t_p for two sheet thicknesses. Debonding initiation stress σ_d is defined as the applied stress that initiates debonding. Obviously, the debonding initiates at the area where σ_d/p_s is smaller. At small values of t_p, the debonding initiates at the crack region while at large ones at the upper patch edge. This is because with decreasing t_p the shear stresses at the patch edge decrease (role of tapering) while those at the crack region increase (the resistance to crack opening is smaller). The transition of debonding initiation from area A to B takes place at larger values of t_p as the sheet thickness increases because the ratio of patch stiffness to the sheet stiffness t_s decreases.

3.2. Effect of adhesive thickness

Fig. 8 shows the variation of σ_d/p_s at the areas A and B as function of the adhesive thickness for two sheet thicknesses. It is evident that increasing the adhesive thickness will increase the strength of the repair. In general, the adhesive thickness does not affect the position of debonding initiation. However, in the case of $t_s = 3$ mm, shown in Fig. 8(b), for an adhesive thickness less than 0.15 mm debonding will initiate at the crack region, whereas, for an adhesive thickness more than 0.15 mm debonding will initiate at the patch edge.

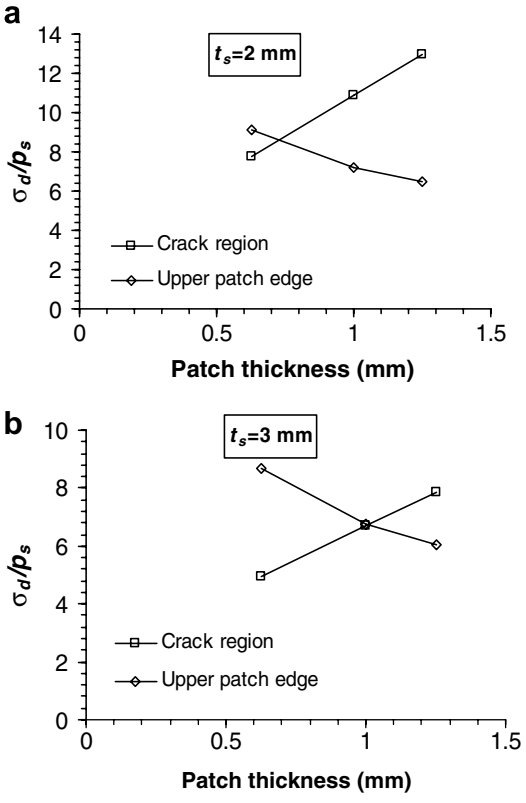

Fig. 7. Variation of (normalized) debonding initiation stress with regard to the patch thickness for two sheet thicknesses.

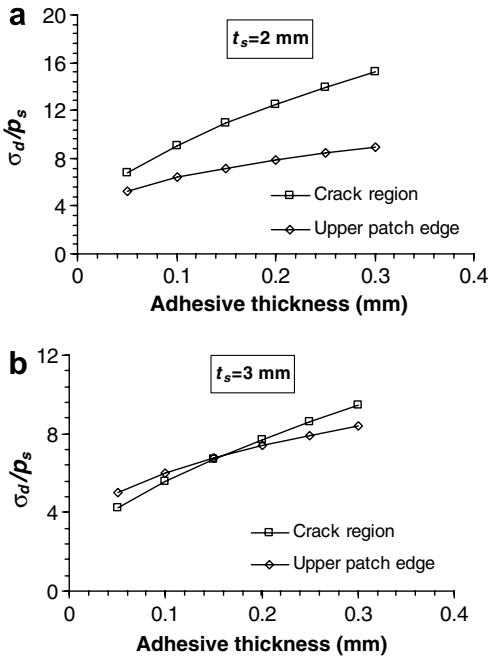

Fig. 8. Variation of (normalized) debonding initiation stress with regard to the adhesive thickness for two sheet thicknesses.

The variation of SIF with regard to the patch thickness and adhesive thickness is shown in Figs. 9(a) and (b), respectively. As can be seen, the trend of variation is opposite. Contrary to patch thickness, the increase in adhesive thickness leads to increase of SIF. This is expected, since a large adhesive thickness will lead to a more resilient repair allowing larger metallic sheet deformation.

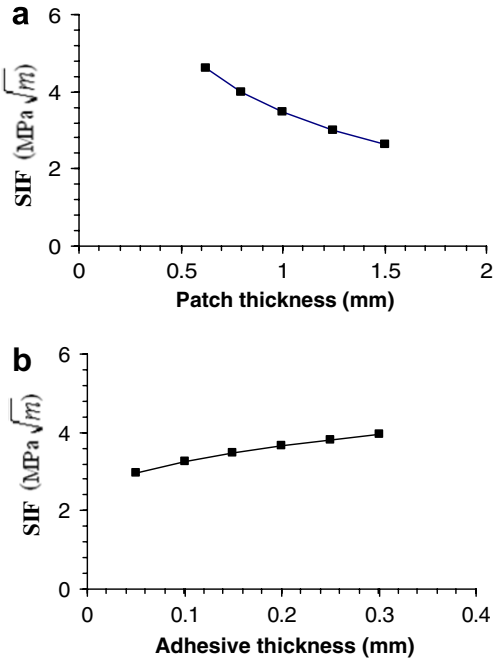

Fig. 9. SIF variation with regard to (a) patch thickness and (b) adhesive thickness.

3.3. Effect of patch width

Figs. 10(a) and (b) show the variation with regard to the patch width of the σ_d/p_s and SIF, respectively. With increasing the patch width, the σ_d/p_s increases at both areas. However, the increase at the upper patch edge where the debonding initiates is insignificant. Therefore, it is concluded that the patch width has a minimal effect on the debonding initiation and zero effect on the debonding progression. On the contrary, it has a considerable positive effect on the SIF.

3.4. Effect of tapered length

Fig. 11 shows the variation of σ_d/p_s with regard to the tapered patch length. As expected, tapering significantly affects the shear stress values at the patch edge but has no effect on the shear stresses at the crack region.

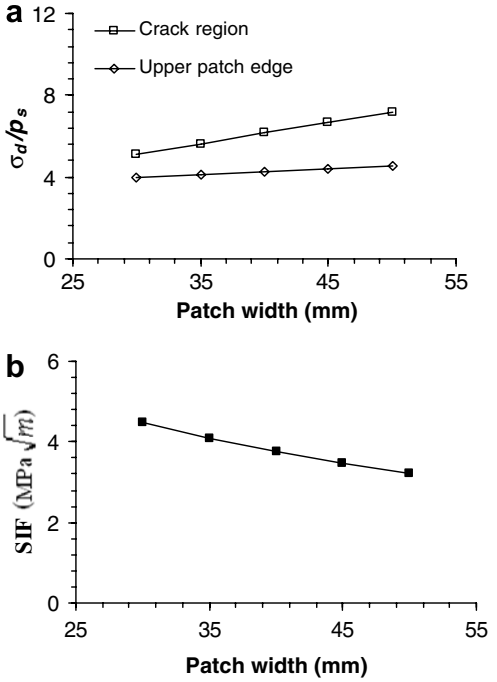

Fig. 10. Variation of (normalized) debonding initiation stress and SIF with regard to the patch width.

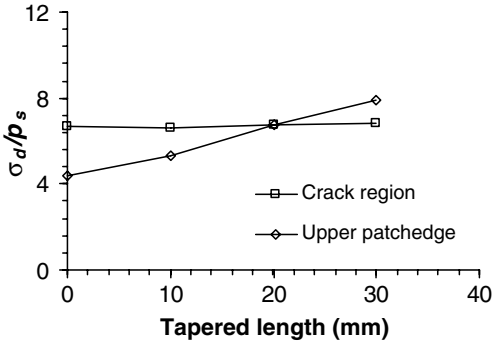

Fig. 11. Variation of (normalized) debonding initiation stress with regard to the tapered length.

4. Debonding initiation and progression

The previous analyses were conducted for a constant applied load. In order to examine the debonding progression, the steps described in the flowchart of Fig. 5 were followed. The first finding was that debonding initiation at the crack region is due to crack opening and it is not catastrophic for the repair in the sense that the load can be increased; the crack must be further opened in order for the debonding to progress. Figs. 12(a) and (b) show the variation of the percent debonded area and SIF with regard to the applied load, respectively, for a case in which debonding initiated at the crack region. The results of Fig. 12 are taken for an adhesive strength $p_s = 40$ MPa. As can be seen in Fig. 12(a), the debonding initiated at 220 MPa. The applied stress continued to increase up to 350 MPa whereat the debonding initiated also at the upper patch edge and propagated instantly leading to complete dissociation of the patch from the sheet. Even though yielding is expected at an applied load of 350 MPa, it should be noted here that the analysis considered in this paper is linear elastic in order to examine the debonding behavior of composite bonded repairs. The SIF, affected by the debonding, increases almost linearly up to the load of 350 MPa whereat it sharply rises from 25 to 73 MPa$\sqrt{m}$. Fig. 13 shows the progression of debonding for this case. The debonding initiated at the crack was confined to the area around it while the debonding initiated later at the upper patch edge propagated very fast.

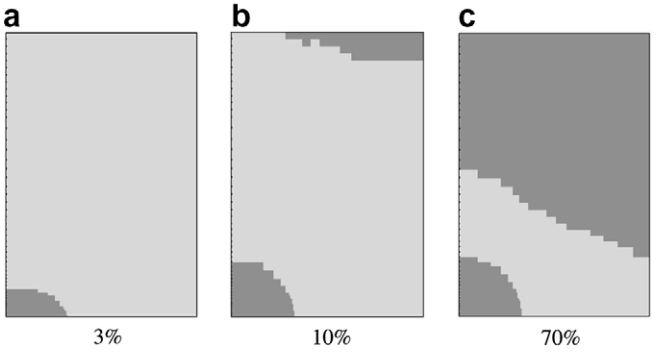

Fig. 13. Increase of the percent debonded area with the applied load for the case of Fig. 12.

On the other hand, when debonding initiates at the upper patch edge, it is catastrophic for the repair because it significantly reduces the patch effective area. In such cases, the debonding initiation load is also the maximum load that the repair can sustain. All iterations are performed under the same load since the criterion of 1% increase of the debonded area is constantly fulfilled (step 8 in the flowchart). Figs. 14(a) and (b) show the variation of the percent debonded area with regard to the number of iterations and the variation of SIF with regard to the percent debonded area, respectively. The results are taken for $p_s = 40$ MPa and the applied load that initiates debonding is 275 MPa. Although the debonded area increases almost linearly with the iterations, the SIF is not affected by this increase except for values of the percent debonded area larger than 86% where it increases sharply. This is

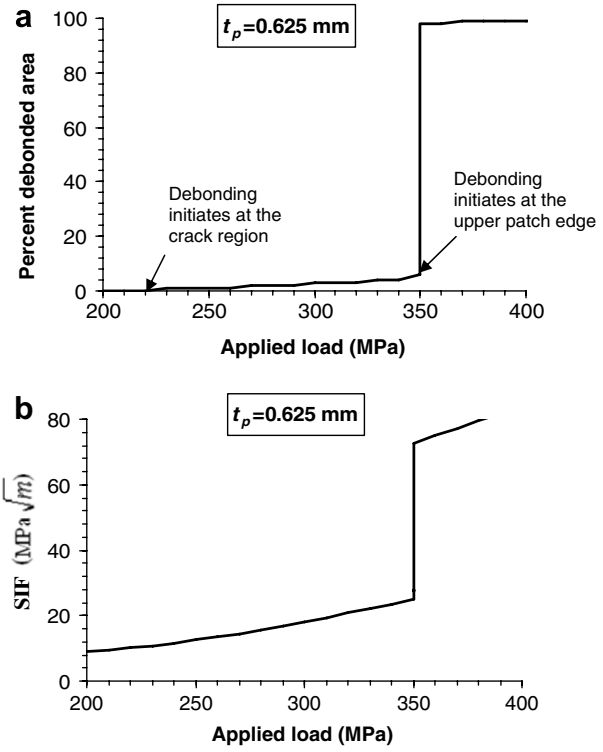

Fig. 12. Progression of debonding (dark grey area) initiated at the crack region.

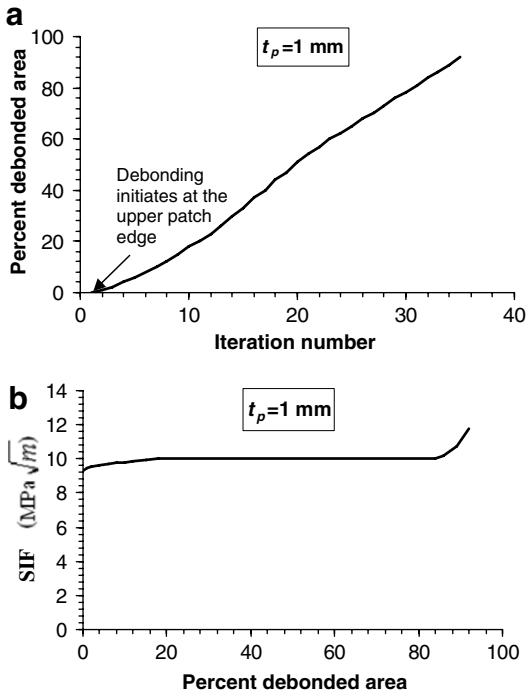

Fig. 14. Progression of debonding (dark grey area) initiated simultaneously at the crack region and the upper patch edge.

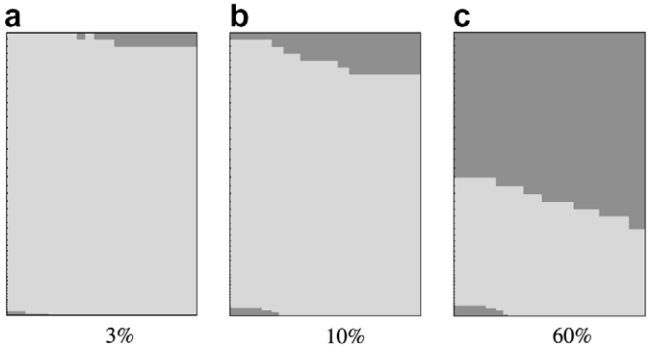

Fig. 15. Increase of the percent debonded area with the applied load for the case of Fig. 14.

due to the debonding of the area of the patch in front of the crack. The progression of debonding for such case is shown in Fig. 15. As can be seen, the debonding soon after the debonding initiated at the upper patch edge, it also did at the crack. However, it propagated faster (at the same load) from the upper edge leading to sudden complete failure of the repair.

5. Discussion and conclusions

In most composite patch repairs of cracked structural elements, patch width and length is controlled not only by the requirements of the crack shielding but also by the position of the repair and care should be taken that no load transfer to neighboring elements takes place. However, patch stiffness and thickness, adhesive thickness and tapered length, are in most situations, chosen from a wide range of possible values. In order for the repair to be efficient, it has to be assured that it will remain in place (no debonding will take place) and that it will reduce the SIF of the crack even below the fatigue threshold values. It should be noted that no effect of the patch elastic properties was considered in this work, since this is equivalent to changing the patch thickness, as the controlling parameter is the product of patch stiffness and thickness.

From the results presented in the previous sections, it was found that the minimum value of the normalized debonding stress σ_d/p_s is about 4. Considering that typical adhesive shear strength is 25–40 MPa [14], this gives a minimum debonding stress of 100–160 MPa. However, careful selections of the repair parameters can double this stress. Therefore, the debonding stress can be much larger than typical maximum fatigue loading, ensuring durability of the repair. However, the effect of environment and loading history on possible degradation of adhesive properties or bondline properties should be also examined. On the other hand, the SIF values evaluated were very small and close to threshold values of Al2024, suggesting that no significant fatigue crack growth will take place.

Ensuring efficiency of the repair, another aspect that it is important is the stress concentration in the metallic plate due to the presence of the patch that occurs just above the patch edge. Considering the typical S–N curve of aluminum alloys used in aircraft structures, an increase of the stress in the metallic plate by, e.g. 10%, might result in approximately 30% reduction in fatigue life. Typical stress concentrations in the metallic plate due to the presence of the patch are shown in Figs. 16(a) and (b). The figures suggest that stress concentration increases with increased patch thickness and decreased adhesive thickness and it ranges between 10% and 15% for the considered repair. Care should be taken that the stress concentration would not cause more damage to the repair area than the original crack itself.

The general conclusion of the present study is that given the adhesive shear strength, patch debonding initiation and progression is controlled by the geometry of the repair. In particular, the following effects have been found:

- At low values of patch thickness, debonding initiates at the crack region, being not catastrophic for the repair, while at large ones it initiates at the upper patch edge, being catastrophic. The transition of debonding initiation from one area to the other depends also on the sheet thickness.
- The increase of patch thickness, adhesive thickness and tapered length results in a significant increase of the debonding initiation stress at the crack region. The effect of patch width has been found to be minimal.

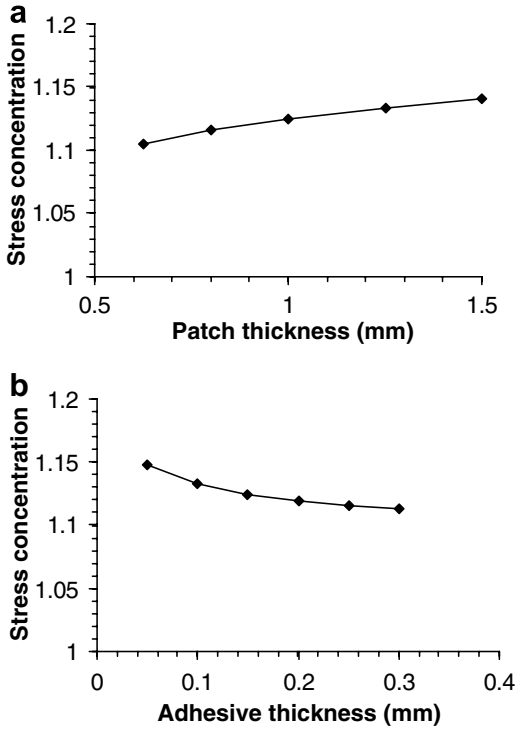

Fig. 16. Stress concentration as function of (a) patch thickness and (b) adhesive thickness.

- Contrary to the adhesive thickness, the increase of patch thickness and patch width results in a decrease of the SIF.

Acknowledgments

The work presented in this paper is part of the work conducted within the frame of the European Research Project 'IARCAS' (Improve and Assess Repair Capability of Aircraft Structures), which focused on the improvement and development of new repair techniques and extension of allowable damages for primary metallic aircraft structures. The financial support provided by the European Commission under Contract G4RD-CT2000-00401 is gratefully acknowledged.

References

[1] GROWTH Project GRD1–2000–25182. Improve and assess repair capability of aircraft structures (IARCAS). Annex I: Description of the Work 2000.
[2] Baker AA, Jones R. Bonded repair of aircraft structure. Hague: Martinus Nijhoff; 1988.
[3] Fredell R, Guijt C, Mazza J. An integrated bonded repair system: A reliable means of giving new life to aging airframes. Appl Compos Mater 1999;6:269–77.
[4] Naboulsi S, Mall S. Characterization of fatigue crack growth in aluminium panels with a bonded composite patch. Compos Struct 1997;37:321–34.
[5] Denney JJ, Mall S. Characterization of debond effects on fatigue crack growth behavior in aluminum plate with bonded composite patch. Eng Fract Mech 1997;57:507–25.
[6] Naboulsi S, Mall S. Modeling of a cracked metallic structure with bonded composite patch using the three layer technique. Compos Struct 1996;35:295–308.
[7] Megueni A, Bachir Bouiadjra B, Belhouari M. Disbond effect on the stress intensity factor for repairing cracks with bonded composite patch. Comput Mater Sci 2004;29:407–13.
[8] Ouinas D, Bouiadjra BB, Serier B. The effects of disbonds on the stress intensity factor of aluminium panels repaired using composite materials. Compos Struct, in press. doi:10.1016/j.compstruct.2005.10.012.
[9] Kermanidis TH, Labeas G, Tserpes KI, Pantelakis SP. Finite element modelling of damage accumulation in bolted composite joints under incremental tensile loading. In: CD–ROM Proceedings of the 3rd ECCOMAS Congress, 11–14 September 2000, Barcelona, Spain.
[10] Papanikos P, Tserpes KI, Pantelakis SP. Modelling of fatigue damage progression and life in CFRP laminates. Fatigue Fract Eng Mater Struct 2003;26:37–47.
[11] Tserpes KI, Papanikos P, Kermanidis Th. A three-dimensional progressive damage model for bolted joints in composite laminates subjected to tensile loading. Fatigue Fract Eng Mater Struct 2001;24(10):673–86.
[12] Papanikos P, Tserpes KI, Labeas G, Pantelakis Sp. Progressive damage modelling of bonded composite repairs. Theoret Appl Fract Mech 2004;63:219–30.
[13] ANSYS 7.1. User's manual. 2004. ANSYS, Inc. Southpointe, Canonsburg, PA 15317, USA.
[14] Shear stress–strain data for structural adhesives. DOT/FAA/AR–02/97. Final Report, Washington DC, 2002.